Romanian Reports in Physics **72**, 201 (2020)

TERNARY FISSION BARRIERS

R. A. GHERGHESCU, D. N. POENARU

Department of Theoretical Physics,
National Institute for Physics and Nuclear Engineering "Horia Hulubei",
Atomistilor 407, RO-077125, POB-MG6, Măgurele-Bucharest, Romania
Email: *radu@theory.nipne.ro*

Received November 24, 2019

Abstract. Ternary fission into three equal fragments is studied within an adapted macroscopic-microscopic method. The Yukawa-plus-exponential potential is used to calculate the charged liquid drop part of the deformation energy. The particular feature is that one calculates the electrostatic and nuclear interaction two by two between the three fragments. For the microscopic part a three center shell model is developed in order to obtain the single particle levels for ternary configuration. The Strutinsky method is then employed to calculate the shell corrections. The ternary fission barriers are obtained by varying the total deformation energy along the distance between the three fragment centers. Calculations are performed for the splitting of ^{144}Nd and ^{210}Po.

Key words: Ternary fission, charged liquid drop, shell corrections, three center shell mode.

1. INTRODUCTION

This work performed calculations which refer to the symmetric ternary fission from light and heavy nuclei. Obviously one agrees to expect poor probabilities, taking into account the fact that binary fission is already favored. The ternay fission was observed by many experimental groups since 1950's. The main feature was that the third particle is a very light one. Such a study is worthy in light of rather recent experiments, like the one published in [1], where the very performant Gammasphere detector was used to report on binary and alpha accompanied ternary fission from ^{252}Cf. Cold alpha and ^{10}Be ternary spontaneous fission pairs have been identified, with the other two fragments more or less symmetric. Other experiments also showed that light-charged particle accompanied ternary fission fragments are detected from ^{252}Cf [2]. In fact ternary fission is recorded from Pu and U since early experiments [3]. Also, long time ago calculations have been performed for ternary fission, refering to fragments with comparable mass [4]. Large prolate deformations are shown to be energetically favored to transform into colinear ternary shapes. The barriers calculated in [4] for Z=114 are low, but only a Q-dependent shell correction energy is taken into account. Theoretically it is demonstrated since longtime ago that triple partition fission is possible and can have, in some cases, comparable probability to

the binary process [5]. Ternary fission came also under scrutiny since early years [6]. The study was made using selfconsistent calculations and ended to the conclusion that binary and ternary fission barriers are comparable in some cases. Our approach has the advantage of including the influence of the fragment shells all along the splitting process. At the beginning, the three body shape could considerably increase the value of the deformation energy, hence the fission barrier.

2. THE TERNARY MACROSCOPIC-MICROSCOPIC METHOD

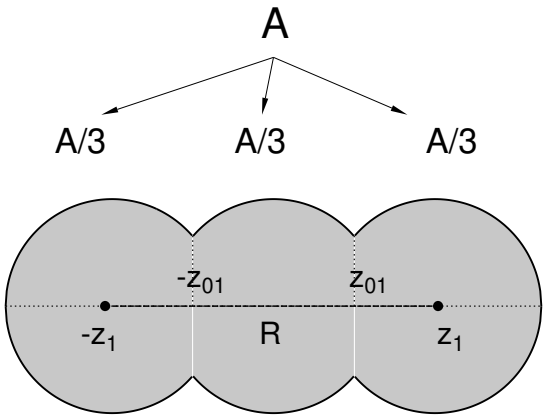

Fig. 1 – Symmetrical ternary fission configuration for a parent nucleus mass A into $A/3$ fragments. The center of the side fragments are mentioned at $-z_1$ and z_1, as well as the separation planes.

The adapted method for the study of ternary fission comprises two main components: the macroscopic part and the microscopic one based on shell effects. The typical shape treated here is described in Fig. 1. It consists of three intersected spherical fragments as being the result of the division of a nucleus with mass A into three A/3 bodies. The distance between the centers of the side fragments is the only degree of freedom, once the parent is fixed. The centers are located at $-z_1$, 0 and z_1 on the symmetry axis Oz. The ternary macroscopic energy is obtained by using the Yukawa-plus-exponential potential to calculate the nuclear surface term and the typical charged liquid drop to obtain the electrostatic part:

$$E_{def} = E_{LDM} + E_{shell} \tag{1}$$

The macroscopic deformation energy for the three part splitting reads:

$$E_{LDM} = E_C + E_{Y+E} \tag{2}$$

where E_C is the Coulomb energy and E_{Y+E} is the nuclear surface part. The Coulomb energy for the three overlapped fragments is calculated as:

$$\begin{aligned} E_C =& \frac{2\pi}{3}(\rho_{eH}^2 F_{C_H} + \rho_{eL}^2 F_{C_L} + 2\rho_{eH}\rho_{eL}F_{C_{HL}} + \\ & \frac{2\pi}{3}(\rho_{eH}^2 F_{C_H} + \rho_{eL}^2 F_{C_m} + 2\rho_{eH}\rho_{em}F_{C_{Hm}} + \\ & \frac{2\pi}{3}(\rho_{el}^2 F_{C_m} + \rho_{em}^2 F_{C_m} + 2\rho_{el}\rho_{em}F_{C_{ml}}) \end{aligned} \tag{3}$$

where ρ_{ei} is the charge density and c_{si} the surface coefficient. F_{C_i} and F_{EY_i} are shape dependent integrals. Every electrostatic interaction term is calculated as:

$$\begin{aligned} & F_C(z,z\prime) = \\ & \left\{\rho(z)\rho(z\prime)\frac{K(k)-2D(k)}{3}\right. \\ & \left[2(\rho^2(z)+\rho^2(z\prime)-(z-z\prime)^2+1.5(z-z\prime)\left(\frac{d\rho^2(z\prime)}{dz\prime)}-\frac{d\rho^2(z)}{dz}\right)\right]+ \\ & K(k)\left\{\frac{\rho^2(z)\rho^2(z\prime)}{3}+\left[\rho^2(z)-0.5(z-z\prime)\frac{d\rho^2(z)}{dz}\right]\left[\rho^2(z\prime)+0.5(z-z\prime)\frac{d\rho^2(z\prime)}{dz\prime}\right]\right\}\Bigg\} \\ & \frac{1}{[(\rho(z)+\rho(z\prime))^2+(z-z\prime)^2]^{1/2}} \end{aligned} \tag{4}$$

where

$$\begin{aligned} k^2 &= \frac{4\rho(z)\rho(z\prime)}{[\rho(z)+\rho(z\prime)]^2+(z-z\prime)^2} \\ D(k) &= \frac{K(k)-K\prime(k)}{k^2} \end{aligned} \tag{5}$$

and $\rho(z)$ is the surface equation. The corresponding integrals are:

$$F_{C1} = \int_{-a_1}^{z_s} dz \int_{-a_1}^{z_s} dz\prime F_1(z,z\prime) \tag{6}$$

$$F_{C2} = \int_{z_s}^{R+a_2} dz \int_{z_s}^{R+a_2} dz\prime F_2(z,z\prime) \tag{7}$$

$$F_{C12} = \int_{-a_1}^{z_s} dz \int_{z_s}^{R+a_2} dz\prime F_{12}(z,z\prime) \tag{8}$$

Correspondingly, the Yukawa-plus-exponential energy E_Y is [7]:

$$\begin{aligned} E_Y =& \frac{1}{4\pi r_0^2}[c_{sl}F_{EYl} + c_{sr}F_{EYr} + 2(c_{sl}c_{sr})^{1/2}F_{EYlr}] \\ & \frac{1}{4\pi r_0^2}[c_{sl}F_{EYl} + c_{sm}F_{EYm} + 2(c_{sl}c_{sm})^{1/2}F_{EYlm}] \\ & \frac{1}{4\pi r_0^2}[c_{sm}F_{EYm} + c_{sr}F_{EYr} + 2(c_{sm}c_{sr})^{1/2}F_{EYmr}] \end{aligned} \tag{9}$$

where the indices stand for left, middle, right, and [8]:

$$\begin{aligned} F_{EY1} &= \int_0^{2\pi}\int_{-a_1}^{z_s}\int_{-a_1}^{z_s} F_{Y1}^{(1)}F_{Y2}^{(1)}Q^{(1)}d\phi dz dz\prime \\ F_{EY2} &= \int_0^{2\pi}\int_{z_s}^{R+a_2}\int_{z_s}^{R+a_2} F_{Y1}^{(2)}F_{Y2}^{(2)}Q^{(2)}d\phi dz dz\prime \\ F_{EY12} &= \int_0^{2\pi}\int_{-a_1}^{z_s}\int_{z_s}^{R+a_2} F_{Y1}^{(12)}F_{Y2}^{(12)}Q^{(12)}d\phi dz dz\prime \end{aligned} \tag{10}$$

The terms in the integrand are:

$$\begin{aligned} F_{Y1}^{(i)} &= \rho_i^2(z) - \rho_i(z)\rho_i(z\prime)cos\phi - 0.5(z-z\prime)\frac{d\rho_i^2(z)}{dz} \\ F_{Y2}^{(i)} &= \rho_i^2(z\prime) - \rho_i(z)\rho_i(z\prime)cos\phi + 0.5(z-z\prime)\frac{d\rho_i^2(z\prime)}{dz\prime} \\ Q^{(i)} &= 2 - \left[\left(\frac{\sigma_i}{a}\right)^2 + 2\frac{\sigma_i}{a} - 2\right]e^{-\frac{\sigma_i}{a}}\cdot\frac{1}{\sigma_i^4} \\ \sigma_1 &= [\rho_i^2(z) + \rho_i^2(z\prime) - 2\rho_i(z)\rho_i(z\prime)cos\phi + (z-z\prime)^2]^{1/2} \end{aligned}$$

with i=l,m,r stands for left, middle and right fragment.

3. THE SYMMETRICAL THREE CENTER SHELL MODEL

The microscopic corrections are obtained as a result of a typical Strutinsky method. The input is the single particle level scheme for a ternary configuration. It is based on the three center oscillator potential, to which the spin-orbit and $\mathbf{l^2}$ terms are added. Due to the axial symmetry, the quantum well is written in cylindrical coordinates as:

$$V_{3osc}(\rho, z) = V(\rho) + V(z) \tag{11}$$

where:

$$V(\rho) = \frac{1}{2} m_0 \omega_\rho^2 \rho^2 \tag{12}$$

and

$$V(z) = \begin{cases} \frac{1}{2} m_o \omega_z^2 (z - z_1)^2, & z > z_{01} \\ \frac{1}{2} m_o \omega_z^2 z^2, & -z_{01} < z < z_{01} \\ \frac{1}{2} m_o \omega_z^2 (z + z_1)^2, & z < -z_{01} \end{cases} \tag{13}$$

z_i are the centers of the three fragments, corresponding to the middle of the potentials. The total Hamiltonian H is written as:

$$H = H_{3osc} + V_{\hat{l}\hat{s}} + V_{\hat{l}^2} \tag{14}$$

where

$$H_{3osc} = -\frac{\hbar^2}{2m_0} \left[\frac{\partial^2}{\partial \rho^2} + \frac{1}{\rho} \frac{\partial}{\partial \rho} + \frac{1}{\rho^2} \frac{\partial^2}{\partial \phi^2} + \frac{\partial^2}{\partial z^2} \right] + V(\rho) + V(z) \tag{15}$$

Since the system is symmetric, the frequencies $\omega_{\rho_1} = \omega_{\rho_2} = \omega_{\rho_3}$. As a result of Hamiltonian separation one obtains the single particle wave functions as:

$$\Psi(\rho, z, \phi) = \Phi_m(\phi) R_{n_\rho}^{|m|}(\rho) Z_\nu(z) \tag{16}$$

where:

$$\Phi_m(\phi) = \frac{1}{\sqrt{2\pi}} \exp(im\phi)$$

$$R_{n_\rho}^{|m|}(\rho) = \left(\frac{2\Gamma(n_\rho + 1)\alpha_1^2}{\Gamma(n_\rho + |m| + 1)} \right)^{\frac{1}{2}} \exp\left(-\frac{\alpha_1^2 \rho^2}{2} \right) (\alpha_1^2 \rho^2)^{\frac{|m|}{2}} L_{n_\rho}^{|m|}(\alpha_1^2 \rho^2)$$

The influence of the tripartition configuration is manifested by the symmetry axis wave functions:

$$Z_\nu(z) = \begin{cases} C_{1n} \exp\left[-\frac{\alpha^2 (z - z_1)^2}{2} \right] \mathcal{H}_\nu[\alpha(z - z_1)], & z \geq z_{01} \\ C_{0n} \exp\left(-\frac{\alpha^2 z^2}{2} \right) [\mathcal{H}_\nu(\alpha z) + (-1)^n \mathcal{H}_\nu(-\alpha z)], & -z_{01} < z < z_{01} \\ (-1)^n C_{1n} \exp\left[-\frac{\alpha^2 (z + z_1)^2}{2} \right] \mathcal{H}_\nu[-\alpha(z + z_1)], & z \leq -z_{01} \end{cases}$$

Within the terms, $L_{n_\rho}^{|m|}$ is the Laguerre polynomial and $\mathcal{H}_\nu$ if the Hermite function. The z-quantum numbers ν, and the constants C_{0n}, C_{1n} are calculated from the normalization and continuity conditions at the separation planes $\pm z_{01}$ between fragments.

The remaining terms of the microscopic potential are the spin-orbit V_{ls} and the l^2 term V_{l^2} .

$$V_{so} = \begin{cases} -\left\{ \dfrac{\hbar}{m_0\omega_0}\kappa_l(\rho,z), (\nabla V_{3osc} \times \mathbf{p})\mathbf{s} \right\}, & A_l - region \\ -\left\{ \dfrac{\hbar}{m_0\omega_0}\kappa_m(\rho,z), (\nabla V^{(r)}_{3osc} \times \mathbf{p})\mathbf{s} \right\}, & A_m - region \\ -\left\{ \dfrac{\hbar}{m_0\omega_0}\kappa_r(\rho,z), (\nabla V^{(r)}_{3osc} \times \mathbf{p})\mathbf{s} \right\}, & A_r - region \end{cases}$$

and

$$V_{\mathrm{l}^2} = \begin{cases} -\left\{ \dfrac{\hbar}{m_0^2\omega_0^3}\kappa_H\mu_H(\rho,z), (\nabla V_{2osc} \times \mathbf{p})^2 \right\}, & A_H - region \\ -\left\{ \dfrac{\hbar}{m_0^2\omega_0^3}\kappa_L\mu_L(\rho,z), (\nabla V_{2osc} \times \mathbf{p})^2 \right\}, & A_L - region \end{cases}$$

The final matrix elements are calculated as:

$$\langle i|3CSM|j\rangle = E_{3osc}(n_\rho, |m|, \nu) + \langle i|V_{\mathbf{\Omega s}}|j\rangle + \langle i|V_{\mathbf{\Omega}^2}|j\rangle \tag{17}$$

where E_{3osc} is the 3-oscillator energy:

$$E_{3osc}(n_\rho, |m|, \nu) = \hbar\omega_\rho(2n_\rho + |m| + 1) + \hbar\omega_z(\nu + 0.5) \tag{18}$$

The diagonalization follows and the final three center single particle energy levels are obtained. The levels are input for the smoothing type Strutinsky method in order to obtain the shell corrections, which are added to the liquid drop deformation energy. As the distance between centers varies, one obtain the ternary fission barrier for symmetric splitting of the decaying nucleus.

4. RESULTS AND DISCUSSION

This work chose two parent nuclei splitting in three equal fragments. The choice has been made so that one can take advantage of proton and neutron shell closures within the fragments.

The first parent nucleus is taken as ^{210}Po, splitting in three equal ^{70}Ni. The shell corrections are displayed in Fig. 2. One can observe the negative total value for the proton part of the shell corrections E_{shp}, due to the closed shell of Z=28 of the Ni nucleus. The negative value of the proton shell corrections comes into lowering the fission barrier. However, the neutron shell part is positive, but rather insignifiant. The negative shell corrections starts to manifest at R=7 fm already. This means that

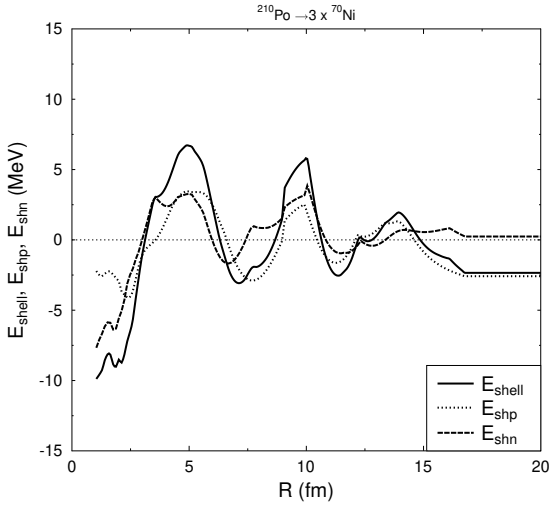

Fig. 2 – Proton, neutron and total shell correction energy for the symmetric ternary splitting of ^{210}Po into three ^{70}Ni fragments.

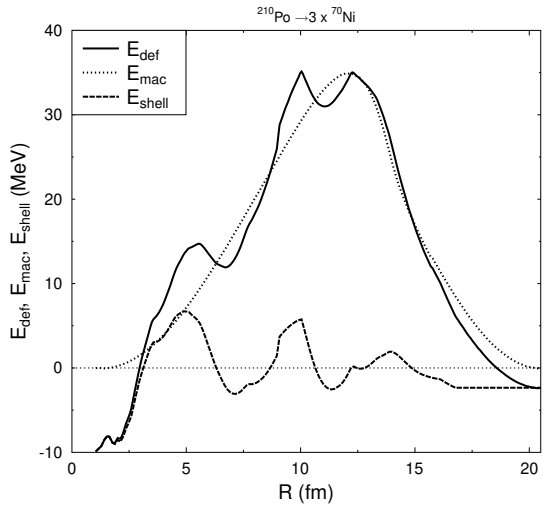

Fig. 3 – Ternary fission shell correction, macroscopic energy and total fission barrier for ^{210}Po parent nucleus.

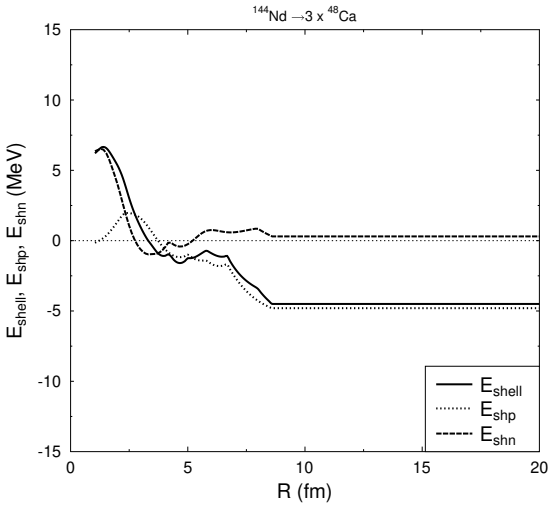

Fig. 4 – Proton, neutron and total shell correction energy for ternary fission of ^{144}Nd. One can observe the minima due to the Z=20 proton magic number of the Ca fragments.

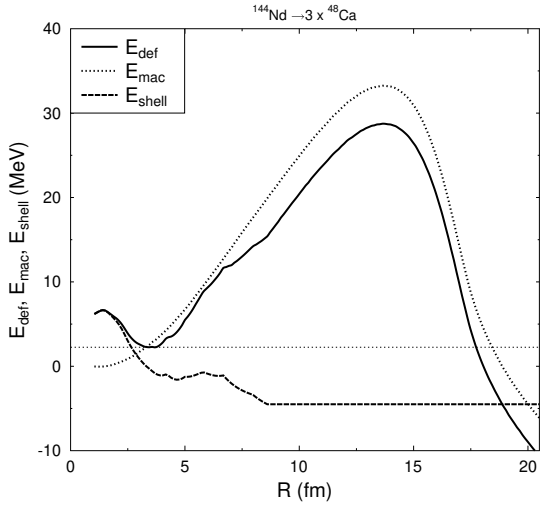

Fig. 5 – Ternary fission shell correction, macroscopic energy and total ternary fission barrier for ^{144}Nd parent nucleus.

the ternary character of the process is present since the three fragments are still overlapped. The total deformation energy, calculated as the sum of the charged liquid drop and the shell corrections, is presented in Fig. 3, for the parent nucleus ^{144}Nd. Two minima due exclusively to the shell correction negative values at a distance between centers R=7 fm, and 11.3 fm (the distance is taken between the left and right fragment centers), are visible on the fission barrier. It gives the possibility to accomodate shape isomers similar to a ternary configuration. However, the macroscopic part of the deformation energy goes up to over 30 MeV. A comparison with binary fission barriers, which are of about 6 MeV for Po, makes ternary fission for this nucleus a much rare phenomenon.

The second parent nucleus is taken to be ^{144}Nd. It has been chosen to take advantage from the double closure of the ^{48}Ca fragments. The Z=20 will provide strong negative shell corrections, thus lowering the final deformation energy. One can see in Fig. 4, that the total shell corrections for completely ternary split is about -5.5 MeV. The proton gap in the fragment level scheme is rather large at Z=20, providing the negative value summed over the three Ca emitted fragments. The macroscopic part for this geometry has a maximum of about 32 MeV. The barrier presented in Fig. 5 spreads over the whole overlapping region.

Though the minima of the shell corrections lowers the deformation energy in a significant way, down to 26 Mev, it still goes to a large value compared to the binary fission barrier. However, it is well known that this is a much less probable phenomenon than the binary fission, so that one can go further with dynamical calculations also for other parent nuclei, in order to chose the best candidate for ternary fission.

Acknowledgements. This work has been supported by the Nucleu Program PN19060101/2019.

REFERENCES

1. A. V. Ramaya *et al.*, Progress in Part. Nucl. Phys. **46** (2001) 221.
2. P. Schall, P. Heeg, M. Mutterer, and J. P. Theobald, Phys. Lett. B **191** (1987) 339.
3. M. L. Muga, C. R. Rice, and W. A. Sedlacek, Phys. Rev. Lett. **18** (1967) 404.
4. H. Schultheis and R. Schultheis, Phys. Lett. B **43** (1974) 423.
5. J. Gruman, U. Mosel, B. Fink, and W. Greiner, Zeit. Phys. **228** (1969) 371.
6. D. Kolb, Phys. Lett. B **65** (1976) 319.
7. D. N. Poenaru, I. H. Plonski, and W. Greiner, Phys. Rev. C **74** (2006) 014312.
8. K. T. Davies, A. J. Sierk, and J. R. Nix, Phys. Rev. C **13** (1976) 2385.